NASA TECHNICAL NOTE

NASA TN D-6929

NASA TN D-6929

STATIC STRUCTURAL TESTS OF A 1.5-METER-DIAMETER FABRIC ATTACHED INFLATABLE DECELERATOR

by Conrad M. Willis and Martin M. Mikulas, Jr.

Langley Research Center
Hampton, Va. 23365

NATIONAL AERONAUTICS AND SPACE ADMINISTRATION • WASHINGTON, D. C. • OCTOBER 1972

STATIC STRUCTURAL TESTS OF A 1.5-METER-DIAMETER FABRIC ATTACHED INFLATABLE DECELERATOR

By Conrad M. Willis and Martin M. Mikulas, Jr.
Langley Research Center

SUMMARY

An investigation has been conducted to determine some of the structural characteristics of an attached inflatable decelerator (AID) for use in the design and construction of future models. Three 1.5-m-diameter models constructed from 60 g/m^2 Nomex cloth were tested at differential inflation pressures up to 103 kN/m^2 to determine meridional tape forces, model burst pressure, and model permeability.

The canopy fabric failed at lower inflation pressures than that predicted by linear membrane theory because of the low-modulus material used for the load-carrying meridional tapes. Permeability increased with increasing internal pressure and decreasing external pressure; thus, external test pressures low enough to produce sonic flow are required for the permeability data to be applicable to most flight conditions. The results indicate that model stresses were near the desired isotensoid condition; however, future designs should consider tape stiffness as well as strength.

INTRODUCTION

An extensive research program has demonstrated the feasibility of using attached inflatable decelerators (AID) for supersonic drag augmentation (refs. 1 and 2). An AID is a lightweight coated fabric canopy which is attached directly to the entry vehicle and inflated by ram air. (See fig. 1.) The AID is stowed in the base of the vehicle and is deployed either by ejecting inlet scoops into the airstream or by using an internally stored inflation gas. A toroidal burble fence is added at the maximum diameter of the canopy to improve subsonic stability. Construction of the AID canopy is similar to that of a parachute in that there are many load-carrying meridional tapes overlaying a fabric. However, the fabric must be coated to maintain proper design inflation pressure with the relatively small ram-air inlets.

The present experimental investigation was conducted to determine some of the structural characteristics of the AID for use in the design and construction of future models. Tests were carried out to determine model permeability, tensile forces in

meridional tapes, and canopy bursting pressure. Information was also obtained on the change in model contour with pressure and on the change of permeability with increased coating on the fabric.

The shape of the AID canopy is calculated from linear membrane theory to provide a uniformly stressed structure when subjected to the aerodynamic loadings expected in flight. (See ref. 1.) Basically, these loadings are the internal pressure recovered by the ram-air inlets, the shape-dependent variable aerodynamic pressure on the front surface, and the base pressure (assumed uniform) aft of the maximum diameter. (See fig. 1.) In a static ground test it would be very difficult to simulate the variable pressure distribution which occurs on the front surface and burble fence of the AID; therefore, only the aft, or constant-pressure, portion of the AID canopy was tested.

The configuration chosen for testing was the same as the 1.5-m-diameter configuration which has been used for numerous wind-tunnel tests in the Arnold Engineering Development Center 16-foot supersonic propulsion tunnel at Mach numbers between 2.0 and 4.75. (See refs. 1, 2, and 3.) The details of the design and methods of construction of these models are reported in references 4 and 5.

SYMBOLS

D	displacement of canopy surface from design surface, measured along surface normal (positive when canopy is larger than design shape), cm
f	tensile force in canopy fabric, kN/m
F_m	tensile force in meridional tape, N
L	length of meridional tape (fig. 2) between inner and outer attachment points, 108 cm
L_c	length of tape from load cell to model inner attachment point, cm
P	model permeability, $dm^3/s/m^2$
p_i	differential inflation pressure across model wall, kN/m^2
p_∞	external pressure on model, kN/m^2
R	model radius, 69.34 cm

r distance from model center line, cm

r_1 radius of canopy inner attachment point, cm

y distance from model reference plane, cm

θ meridian angle for locating points on model, rad

MODELS AND APPARATUS

Models

A cutaway drawing of a complete AID installed on an entry body is presented in figure 1. The test models represent only the aft portion of the AID from the burble fence to the inner attachment point at the minimum diameter. A sketch of the model and test fixture showing dimensions and material specifications is presented in figure 2, and a photograph of the inflated model is presented in figure 3. The models were 138.68 cm in diameter. This diameter is equal to that for the models of reference 3 excluding the burble fence. The models were made from 16 gores of coated Nomex cloth reinforced by 48 meridional Nomex tapes. The basic cloth weighed 60 g/m^2 and was coated with 20 g/m^2 of Viton. The cloth uniaxial tensile strength was 16 kN/m in the warp direction and 15 kN/m in the fill direction. The tapes were 0.7 cm wide and had a tensile strength of 2.5 kN. Both the inner and the outer edges of the model were folded around a 0.5-cm dacron cord in order to keep the canopy from slipping through the mounting clamp when loaded. All model seams were of sewn construction. Model mass was about 0.98 kg and the surface area was 2.29 m^2 (area under clamps not included).

Four models were tested. Models 1 and 2 were fabricated with the warp and fill yarns at an equal angle to the model perimeter (gores cut on the bias). Model 3 had the warp yarns perpendicular to the perimeter (unbiased). The fourth model, 1A, was a modification of model 1; after testing model 1 to failure, the failed area was repaired and all meridional tapes were reinforced by sewing a second tape of the same strength over the original tape.

Apparatus and Instrumentation

A schematic diagram of the model and test apparatus is presented in figure 4. A heavy steel safety cover was placed over the model during high-pressure tests. Some of the tests were conducted inside an 18-m-diameter vacuum sphere to simulate the low external pressures at high-altitude design conditions. Dry air at a pressure of 2 MN/m^2 was supplied by a pipe with an inside diameter of 2 cm. The models were mounted on a

conical steel fixture for testing. Annular bands that clamped the canopy against a rubber O-ring on the pressure vessel were used to retain and seal the inner and outer perimeters of the model.

Permeability instrumentation.- Two turbine flowmeters having capacities of 2.5 and 47 dm^3/s located in the high-pressure supply line were used to measure the volumetric flow rate of air entering the model. (See fig. 4.) Air temperature and pressure inside the model and at the flowmeters were measured by using chromel-alumel thermocouples and differential pressure transducers. Ambient laboratory pressure was read from an aneroid barometer.

Tape-force instrumentation.- Tensile forces acting on the meridional tape were measured at several locations by attaching calibrated strain-gage load cells to the tapes and severing the tape to assure that the load cell carried the full tape load. Gage locations and the method of attachment are shown in figure 5. Load-cell output was monitored on auxiliary readout equipment at the test facility and transmitted to a central data-reduction system to be recorded.

Canopy coordinates.- The displacement of the canopy surface from the nominal design coordinates was measured for a range of inflation pressure by using probes contacting the outer surface, as shown in figure 6. Probe displacement was measured by a hand-held scale at low pressures, and a displacement transformer was used to obtain remote readings at the higher pressures.

TESTS

Models 1 and 1A

Model coordinates were measured on model 1 for inflation pressures up to 14 kN/m^2 to determine the accuracy of fabrication and the variation in shape with inflation pressure. Permeability and tape-force data were measured for inflation pressures up to 43 kN/m^2, the maximum obtainable pressure for the flow available from the existing air supply line. The model was then coated with additional Viton to reduce permeability further and thus allow data for higher inflation pressures to be obtained. Inflation pressure was then increased in increments until the bursting pressure was reached. The permeability data for additional coating and the model coordinate date are presented in the appendix.

Model 1A (model 1, repaired and modified) was provided with an oversized, 0.03-mm-thick, plastic membrane liner to permit higher inflation pressures with the existing air supply. Tape-force data were then obtained up to the bursting pressure.

Model 2

Only permeability data were obtained for model 2 for inflation pressures up to 28 kN/m^2 with external pressures ranging from about 0.14 to 102 kN/m^2.

Model 3

Permeability and tape-force data on the unbiased model were obtained for inflation pressures up to 28 kN/m^2. A plastic liner similar to that used for model 1A was then inserted, and tape-force data were obtained up to the burst pressure.

RESULTS AND DISCUSSION

Model Failure

Models 1 and 3 were pressurized to canopy failure. These failures occurred as tears in the fabric; the tapes remained undamaged. The locations of the fabric failures are shown in figure 7 and photographs of the failures are shown in figure 8. Models 1 and 3 failed by tears that passed underneath a load cell, but there was no load cell near the failure in model 1A. Model 1 failed by tears along a warp and a fill yarn that intersected at a tape. The tears extended across both lobes adjacent to the tape. Model 1A failed with a zigzag tear confined to one lobe, but extending from the inner to the outer attachment point.

Model 3 failed by a fabric tear perpendicular to the tape (along a fill yarn) that extended across two lobes.

Canopy Load Distributions

Forces in meridional tapes.- The forces measured in the meridional tapes of models 1, 1A, and 3 are presented in figures 9(a), 9(b), and 9(c) as a function of pressure. The key at the top of each figure gives the meridional and circumferential location of each load cell. Although there is some indication from the data presented in these figures that the meridional tape load decreases toward the outer attachment point, for the most part the variation in these measurements is considered scatter and reflects the amount of error that exists in the model construction and mounting.

In figure 9(d) the average tape forces for the three models are compared with the tape force predicted by linear membrane theory. It should be noted that the force predicted by linear membrane theory depends only on initial geometry and neglects structural stiffness, so that the theoretical result shown holds for all three models. The geometry of the present models (including lobing) was chosen so that the meridional tapes would

carry 97 percent of the meridional load, with the remainder carried by the fabric. (See ref. 4.) This high percentage of loading in the tapes can only be achieved if the lobing in the fabric assumes the design shape.

It can be seen in figure 9(d) that for model 1 and model 3 the measured tape force is considerably below that predicted by linear membrane theory. For these models the decrease in tape force below the predicted level is due primarily to stretching of the tapes, which transfers part of the load to the fabric. This hypothesis is verified by observing the increase in tape force produced by the stiffer double tapes used for model 1A.

Fabric loads.- To obtain further insight into the behavior of these models, fabric loads were obtained from vertical equilibrium of forces on the canopy. Figure 10 presents a free-body diagram of a canopy cross section. In this diagram the fabric load f is assumed to be constant throughout the canopy. It is also assumed that the meridional tape force F_m is a constant. These assumptions are consistent with those used in reference 4 to obtain this particular canopy shape. Enforcing vertical equilibrium on the cross section shown in figure 10 leads to the following equation for the fabric load f:

$$f = \frac{1}{2}\left[p_i\left(R - r_1\right) - \frac{96F_m}{10^3\pi\left(R + r_1\right)}\right] = 0.303p_i - 0.0196F_m \qquad (1)$$

The fabric loads calculated from equation (1) by making use of the average measured tape loads F_m are presented in figure 11. The tape loads from figure 9(d) are repeated in this figure for comparison. The ordinate scale for the fabric loads is on the right of the figure. The theoretical value of the fabric load as given by linear membrane theory (ref. 4) is indicated by the lower dashed line. It can be seen that in the high-pressure range the actual canopy loads are significantly higher than those predicted by linear membrane theory. This overloading of the fabric is due to excessive stretching of the tapes, which is not considered in linear membrane theory.

As can be seen in figure 11, the measured tape loads at burst were lower than the predicted value from linear membrane theory. Since the decrease in tape load must be absorbed by the fabric, the fabric loading was higher than that predicted by linear membrane theory, as shown by the three solid lines in figure 11. It should be noted that the fabric loads presented in figure 11 are only average loads and that higher local loads would exist. This is probably the reason why model 3 had a 13-percent-lower burst pressure than model 1. It is believed that the biased fabric of model 1 permits the fabric to rack and relieve high local fabric loads.

To illustrate the influence of meridional tape stiffness on model integrity, the fabric of the failed model 1 was repaired and all meridional tapes were doubled to increase stiffness. The model was tested to burst pressure as model 1A. As can be seen in figure 11,

the double tapes carried significantly more load than the single tapes and the burst pressure was increased by 15 percent. Unfortunately, sewing the second tape onto model 1 severely degraded the fabric breaking strength because of the more than usual number of needle punctures. Thus, although model 1A had the highest burst pressure, the fabric actually failed at a lower fabric load level. It is expected that if a new canopy were made with tapes as stiff as the tapes on model 1A, a much higher burst pressure could even be achieved. These results indicate that in future designs with this type of construction, both stiffness and strength should be considered in selecting a tape material. The proper tape stiffness needed for an efficient decelerator design can only be determined through the use of a nonlinear membrane theory which takes structural flexibility into account.

Permeability

The permeability of the three models at sea-level external pressure is presented in figure 12. The permeability for very low inflation pressures is shown separately (fig. 12(a)) to permit a comparison with the values obtained at a differential pressure of 0.124 kN/m^2 (0.5 inch of water) generally used in material specifications. References 6 and 7 report measurements of near zero permeability $(1 \times 10^{-3}\ dm^3/s/m^2)$ for a sample of similar material. This large difference between the permeability of a standard specimen of the material and that for a structure made from the material is believed to be due mainly to leakage through needle holes at the seams.

Model 1 (fabric cut on bias) and model 3 (unbiased) had the same permeability (within the accuracy of the instrumentation) throughout the test range of inflation pressure (fig. 12(b)). Model 2 had a permeability about 65 percent of that for the other two models. The difference between models 1 and 2 is possibly due to minor differences in techniques used in coating the fabric and constructing the model.

Figure 13 presents the model permeability for external pressures ranging from 0.14 to 102 kN/m^2. The permeabilities for all values of external pressure p_∞ appear to have a tendency to converge in the region near the value of pressure ratio required for sonic flow through the yarn interstices, that is, $\frac{p_i + p_\infty}{p_\infty} = 1.9$. At lower pressure ratios the flow is subsonic, and permeability is highly dependent upon external pressure. For example, with an inflation pressure of $p_i = 10\ kN/m^2$, a value suitable for some earth atmosphere reentry missions, the measured permeability for model 2 (fig. 13) with sea-level external pressure $(p_\infty = 102\ kN/m^2)$ was only 55 percent of the value measured at external pressures low enough to produce sonic flow $(p_\infty \leq 5\ kN/m^2$ for this inflation pressure). Since most flights are expected to occur in environments that would produce sonic flow through the yarn interstices, permeability data measured in the subsonic flow region would not be meaningful. Additional parameters affecting permeability are interstice size and interstice discharge coefficient. In the sonic flow region external pressure

has less effect on permeability because the flow velocity is constant and the discharge coefficient is less sensitive to external pressure because of the higher Reynolds number. Therefore, above pressure ratios of 1.9 acceptable ground-test permeability data can be obtained without controlling the canopy external pressure. If test results are to be applied to models having various sizes, the permeabilities should be equal when the models have the same fabric stresses rather than when they have the same inflation pressure.

CONCLUSIONS

A static test program of the aft portion of a 1.5-m-diameter attached inflatable decelerator (AID) constructed from Viton coated Nomex fabric has been conducted to determine its meridional tape forces, burst pressure, and permeability. Results from these tests have led to the following conclusions:

1. Meridional tapes used in the original configuration had an undesirably high elongation under load. Increasing the stiffness of the tapes reduced the fabric stress and resulted in a substantial increase in model burst pressure.

2. Linear membrane theory does not adequately describe the behavior of such relatively complex doubly curved structures, and a nonlinear theory that includes structural stiffness should be used.

3. Permeabilities determined at the standard pressure for materials tests, 0.124 kN/m^2 (0.5 inch of water), have little value for evaluating AID performance because the higher fabric stresses at operational conditions produced permeabilities that are generally several orders of magnitude higher than the standard test.

4. Model permeability tests must be conducted with external pressures low enough to produce sonic flow through the yarn interstices in order to obtain data that is meaningful for flight conditions.

Langley Research Center,
National Aeronautics and Space Administration,
Hampton, Va., September 5, 1972.

APPENDIX

PERMEABILITY DATA FOR ADDITIONAL COATING, AND MODEL COORDINATE DATA

The present investigation was conducted primarily to determine the permeability and the meridional tape forces of an AID. Some supplementary information obtained during the investigation is presented in this appendix.

Effect of Additional Fabric Coating on Model Permeability

The effect of fabric coating on model permeability is shown in figure 14. It should be noted that the coating was added because the capacity of the existing air supply line was not sufficient to determine the burst pressure for an uncoated model. Since the only object of the modification was a decreased permeability, the results are not optimum with regard to weight, but in the absence of other data can be regarded as a very conservative indication of the amount of improvement that can be expected from this amount of coating.

The liquid Viton coating was brushed on the outer surface of the model while a low inflation pressure (less than 0.15 kN/m^2) was maintained. The permeability after the additional coating was about 39 percent of the original value. This low permeability was achieved by adding 415 g/m^2 (20 g/m^2 at weaving, 395 g/m^2 after model fabrication) of Viton to a 60 g/m^2 fabric, and changes in the fabric should probably be considered before applying this much coating to a flight article.

AID Coordinates for a Range of Loads

Coordinates of model 1 were measured at several inflation pressures to determine the fabrication accuracy and the amount of model deformation under pressure.

Figure 15 presents the deviation of the canopy surface from the design shape measured normal to the surface for an inflation pressure of 13.8 kN/m^2. At this pressure, which is higher than the operating pressure for some mission profiles, all the meridional tapes (fig. 15(a)) and most of the remainder of the model surface (fig. 15(b)) were inside the design contour. Maximum deviation of meridional tapes from the design contour occurred at about $r/R = 0.7$ and ranged from $D/R = -0.019$ to -0.028 for the six tapes measured. The fabric between the tapes was intended to be lobed, but the coordinates were compared with tape design coordinates to simplify presentation of the data. The lobes were highest near the outer ends of the gore seams (fig. 15(b)).

Measurements made at $r/R = 0.7$ for a few tapes on models 2 and 3 indicated they were also undersized by about the same amount as model 1; however, the lobes between

tapes were lower and flatter for the unbiased fabric used in model 3. This difference in lobe height can be seen in the photographs presented in figure 16.

The difference between the design coordinates and the actual model shape at several inflation pressures is shown in figure 17. The model became somewhat larger than the design contours before reaching burst pressure. The data presented in this figure are for the initial pressurization of the model, and since a substantial portion of the deformation is permanent, subsequent pressurizations would produce smaller changes in shape for a given increment of inflation pressure.

REFERENCES

1. Mikulas, Martin M., Jr.; and Bohon, Herman L.: Development Status of Attached Inflatable Decelerators. J. Spacecraft & Rockets, vol. 6, no. 6, June 1969, pp. 654-660.

2. Bohon, Herman L.; and Miserentino, R.: Attached Inflatable Decelerator Performance Evaluation and Mission-Application Study. AIAA Paper No. 70-1163, Sept. 1970.

3. Bohon, Herman L.; and Miserentino, R.: Deployment and Performance Characteristics of 5-Foot Diameter (1.5 m) Attached Inflatable Decelerators From Mach Number 2.2 to 4.4. NASA TN D-5840, 1970.

4. Barton, R. Reed: Development of Attached Inflatable Decelerators for Supersonic Application. GER-13680 (Contract No. NAS 1-7359), Goodyear Aerospace Corp., May 22, 1968. (Available as NASA CR-66613.)

5. Faurote, G. L.: Design, Fabrication, and Static Testing of Attached Inflatable Decelerator (AID) Models. GER-14940 (Contract No. NAS 1-9726), Goodyear Aerospace Corp., Mar. 1, 1971. (Available as NASA CR-111831.)

6. Deaton, Jerry W.: Air Permeability Studies of a Lightweight Coated Fabric Subjected to Uniaxial Tensile Loads With and Without Prior Cycling. NASA TN D-5931, 1970.

7. Skelton, J.; and Abbott, N. J.: Effect of Strain Rate and Load Cycling on the Tensile Behavior and Air Permeability of a Coated Fabric. Contract No. NAS 1-9816, Fabric Research Laboratories, Inc., [1971]. (Available as NASA CR-111883.)

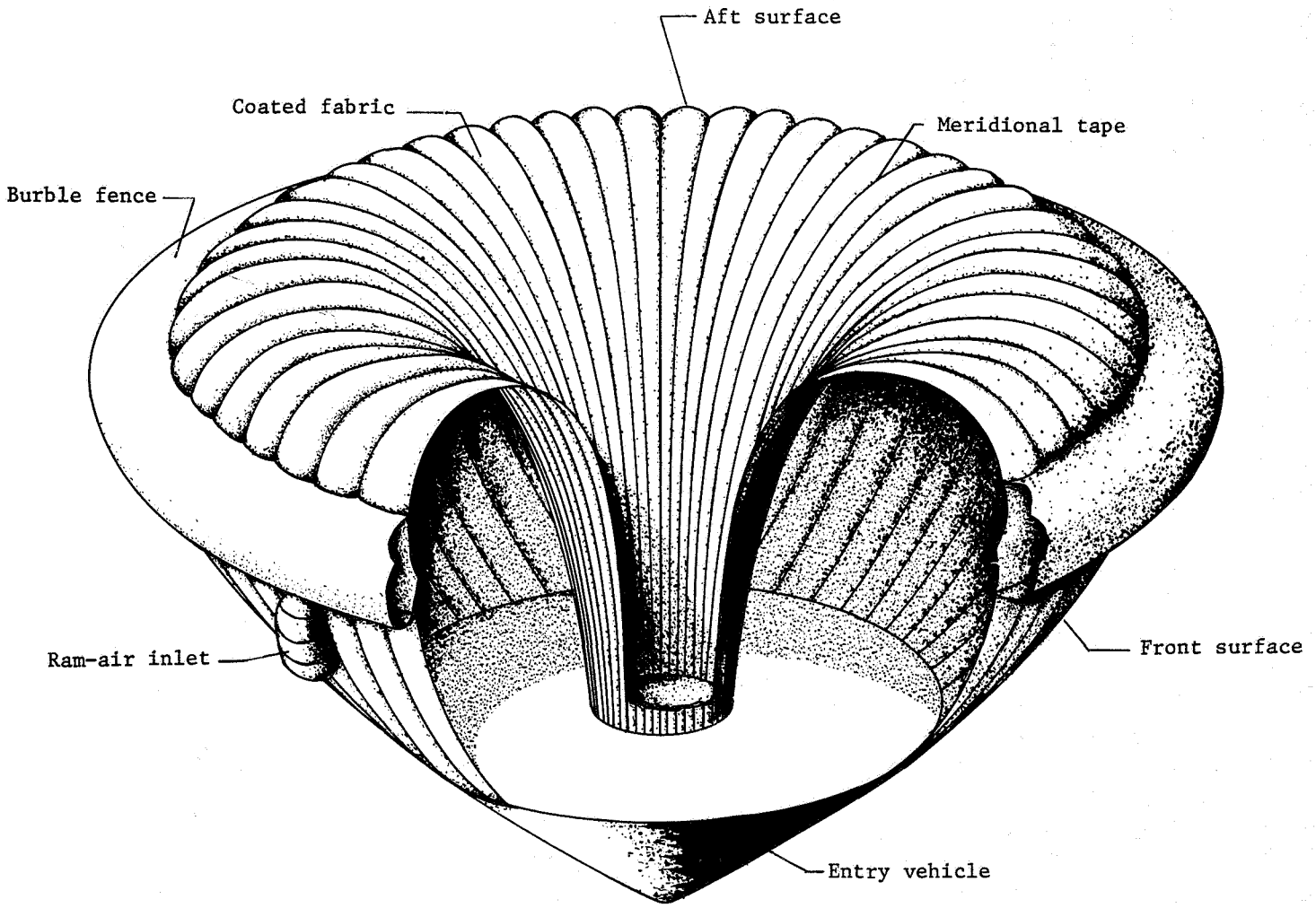

Figure 1.- Cutaway view of attached inflatable decelerator (AID) installed on entry vehicle.

AID Coordinates (ref. 4)	
$\frac{r}{R}$	$\frac{y}{R}$
.1263	.0918
.1260	.1370
.1520	.3702
.1928	.5161
.2377	.6204
.2936	.7136
.3458	.7789
.4389	.8616
.5310	.9126
.6256	.9395
.6850	.9442
.7299	.9414
.7872	.9292
.8603	.8963
.9161	.8524
.9404	.8248
.9820	.7508
1.0000	.6522
.9978	.6033

MODEL DESCRIPTION	
AREA	2.29 m^2
MASS	Model 1 = 0.97 kg, model 2 = 0.98 kg Model 3 = 0.99 kg
FABRIC	60 g/m^2 Nomex with 20g/m^2 Viton coating Tensile strength: warp 16 kN/m, fill 15 kN/m
TAPE	2.5 kN Nomex, 1.4 cm wide but folded before sewing to fabric

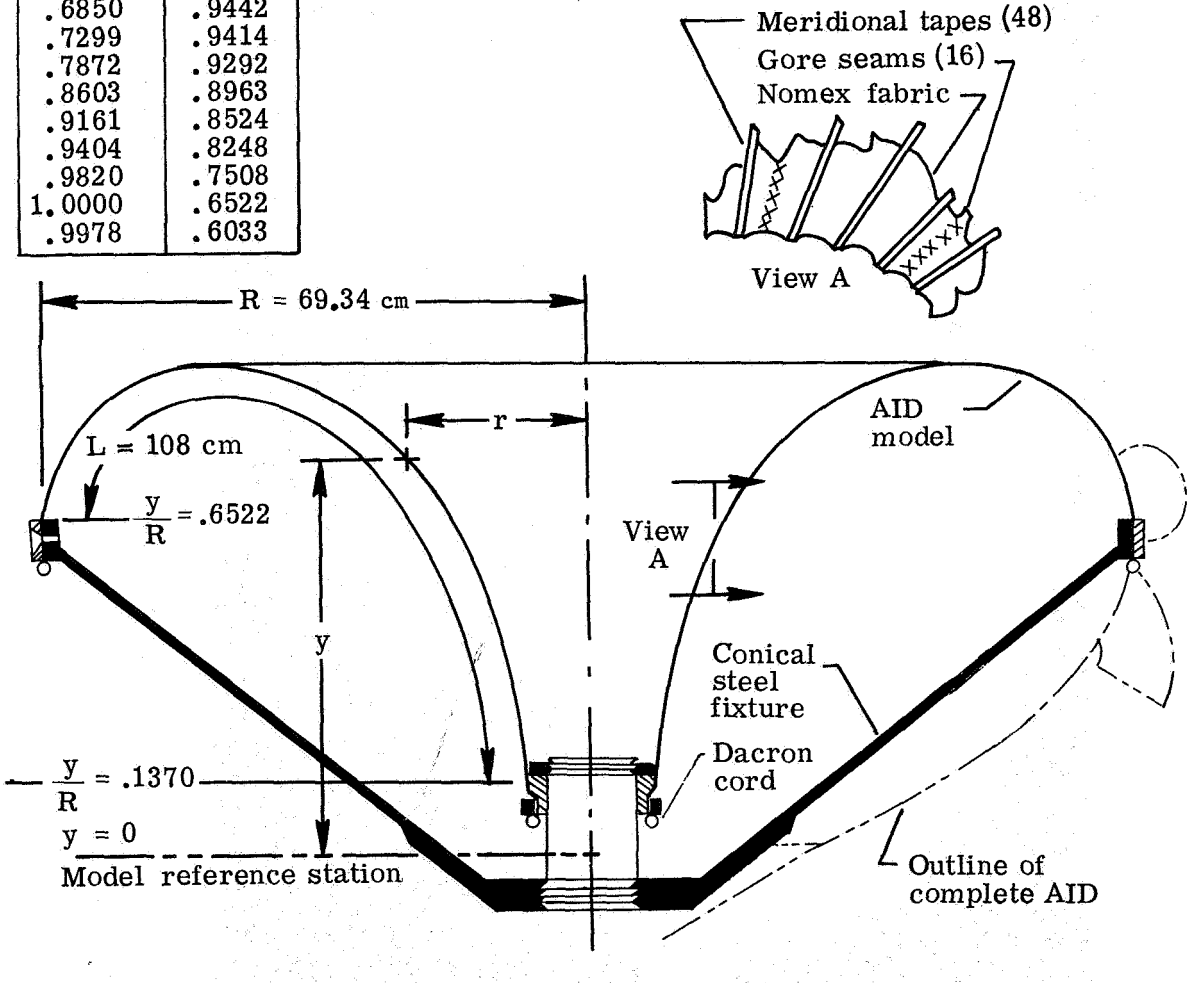

Figure 2.- Cross-sectional sketch of AID model and test fixture.

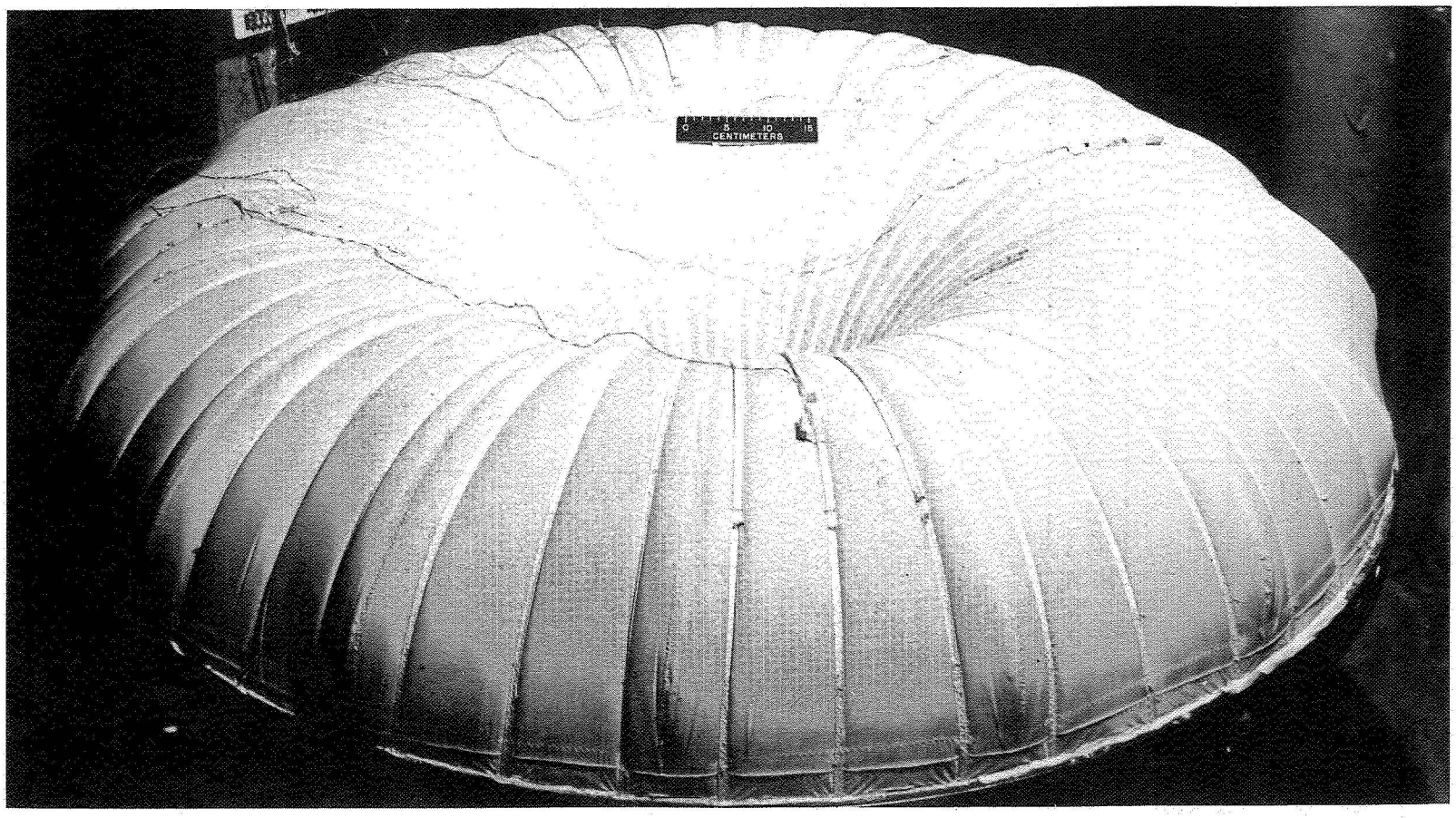

L-70-7090

Figure 3.- Photograph of AID model inflated to 7 kN/m^2.

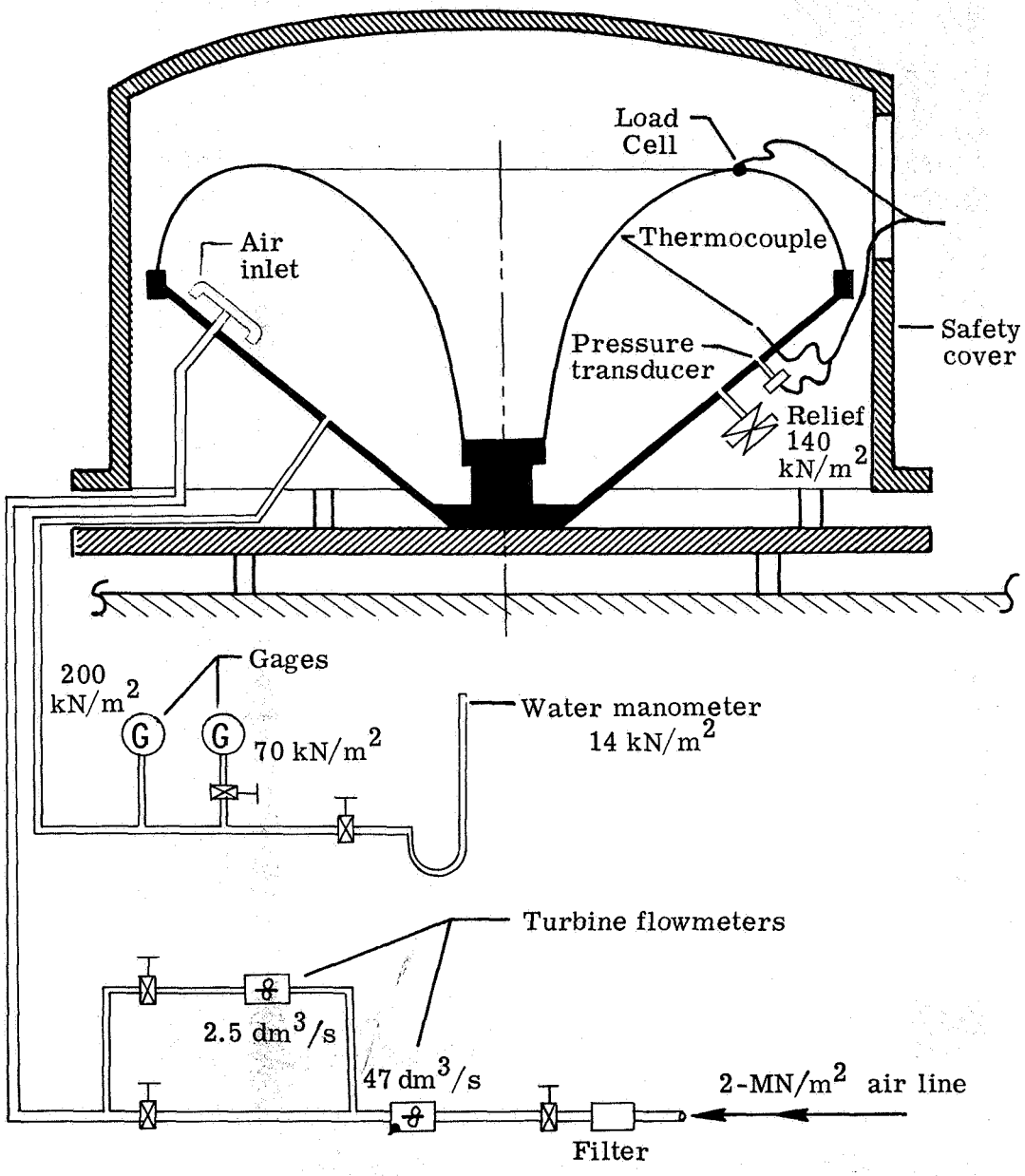

Figure 4.- Schematic of model and apparatus.

Model	Load cell	Meridian angle, θ	Meridional distance, L_c/L
1	1	0.00	.76
	2	1.05	.55
	3	1.18	.55
	4	1.57	.88
	5	1.96	.39
	6	4.32	.13
1A	7	1.31	.75
	8	2.62	.25
	9	2.88	.75
	10	3.27	.25
	11	5.37	.75
3	12	0.00	.65
	13	1.70	.65
	14	2.36	.65
	15	3.27	.65
	16	4.71	.65

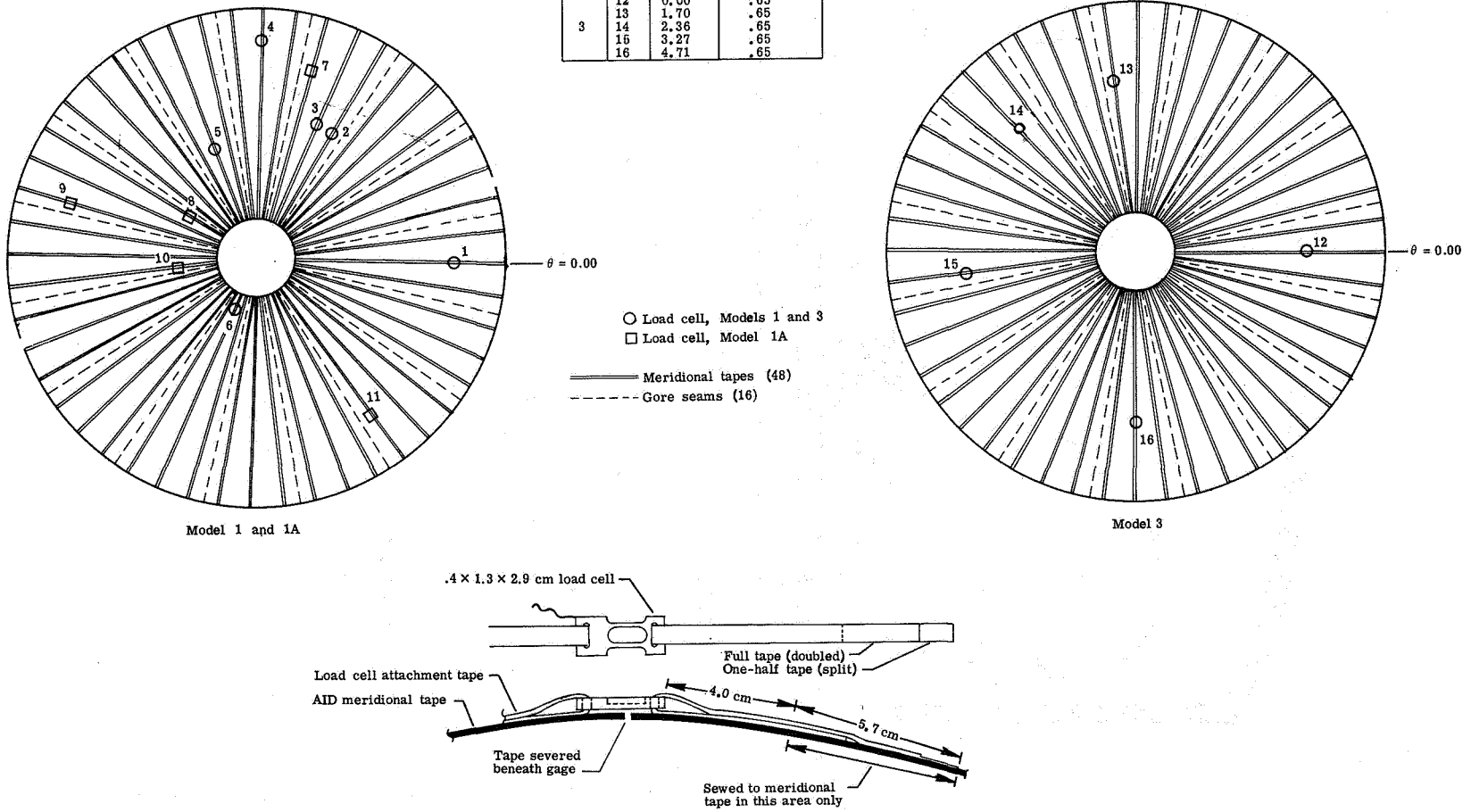

Figure 5.- Location and method of attachment of load cells.

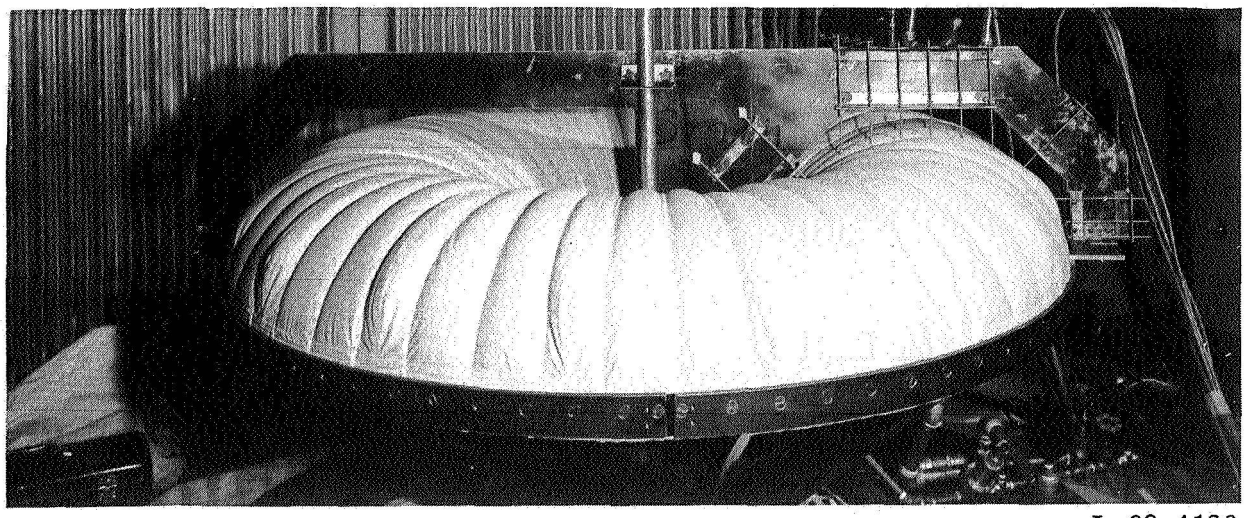

L-69-4126

(a) Probe height read from scale at low pressures.

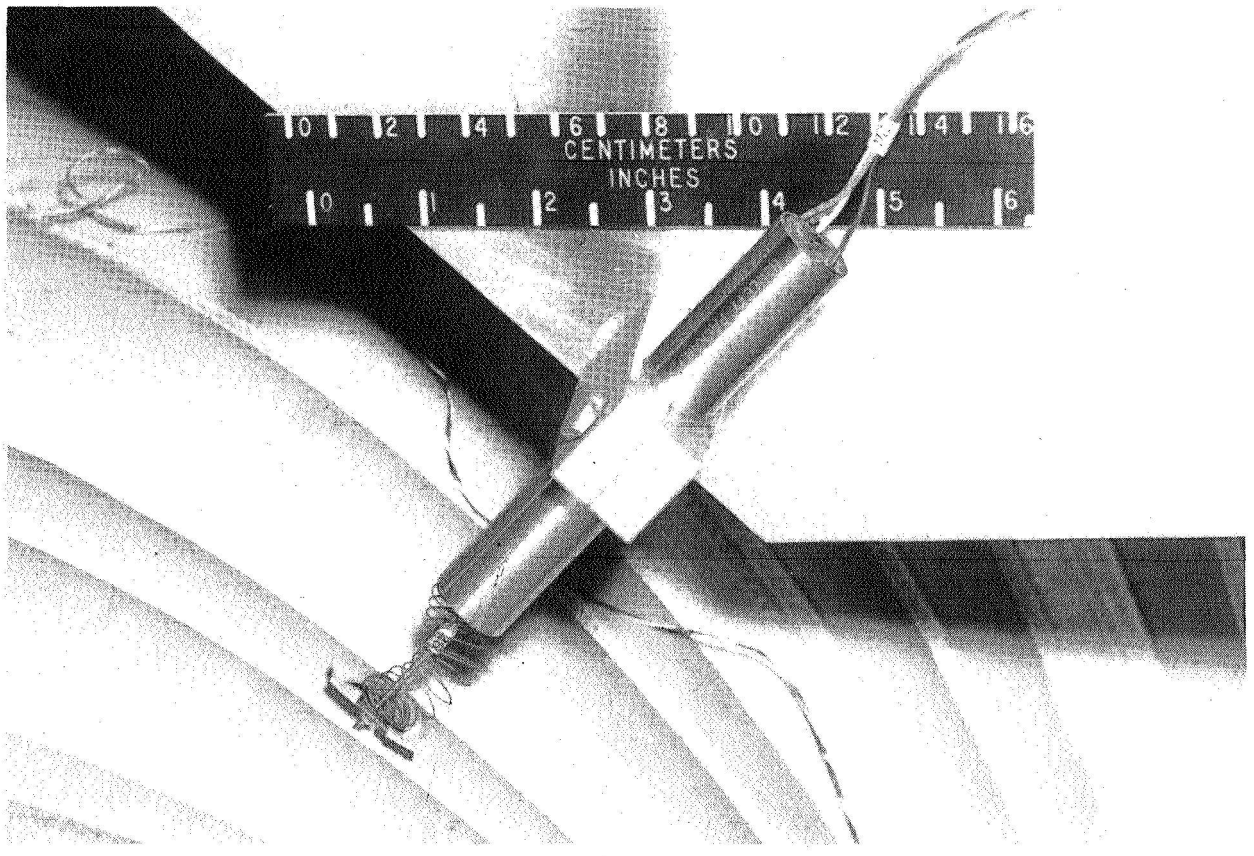

L-69-6184

(b) Displacement transformer for remote measurement at higher pressures.

Figure 6.- Apparatus for measurement of canopy shape.

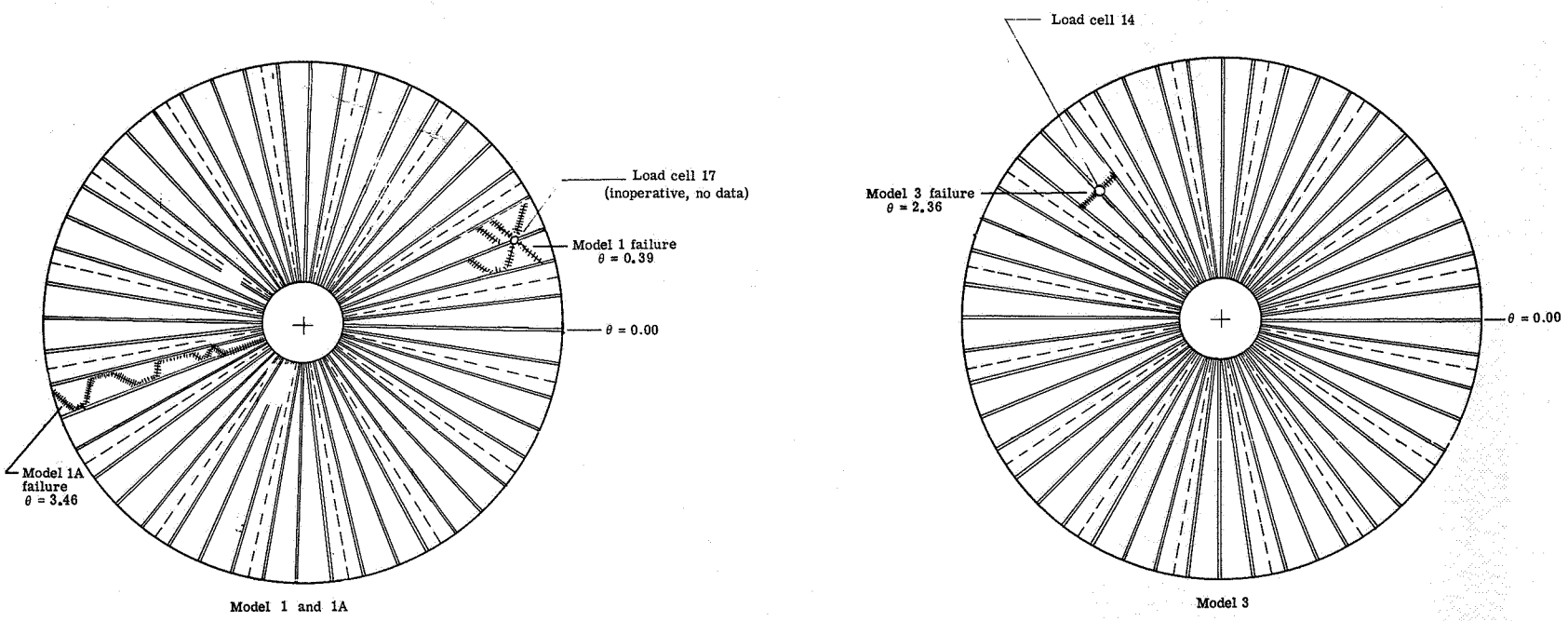

Figure 7.- Location and shape of canopy failure.

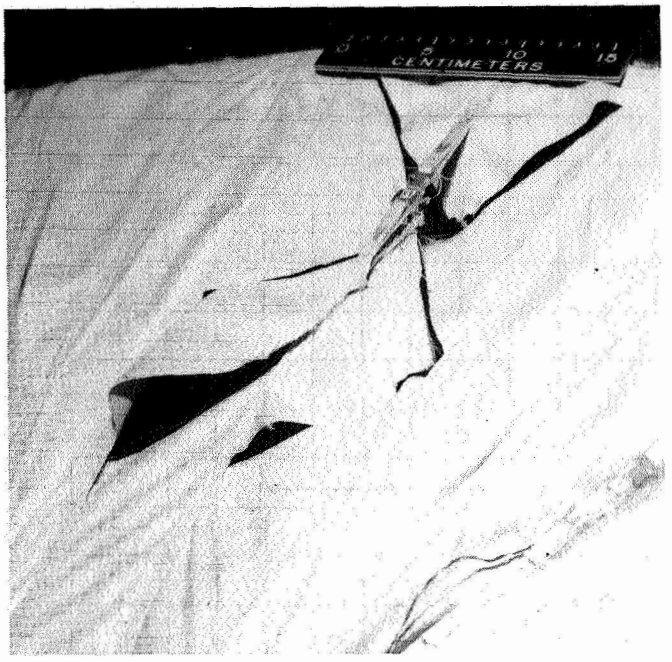

Model 1

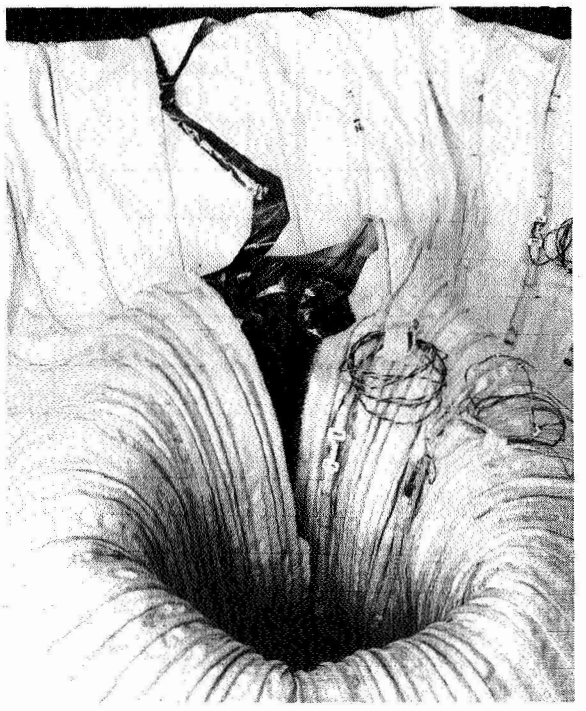

Model 1A

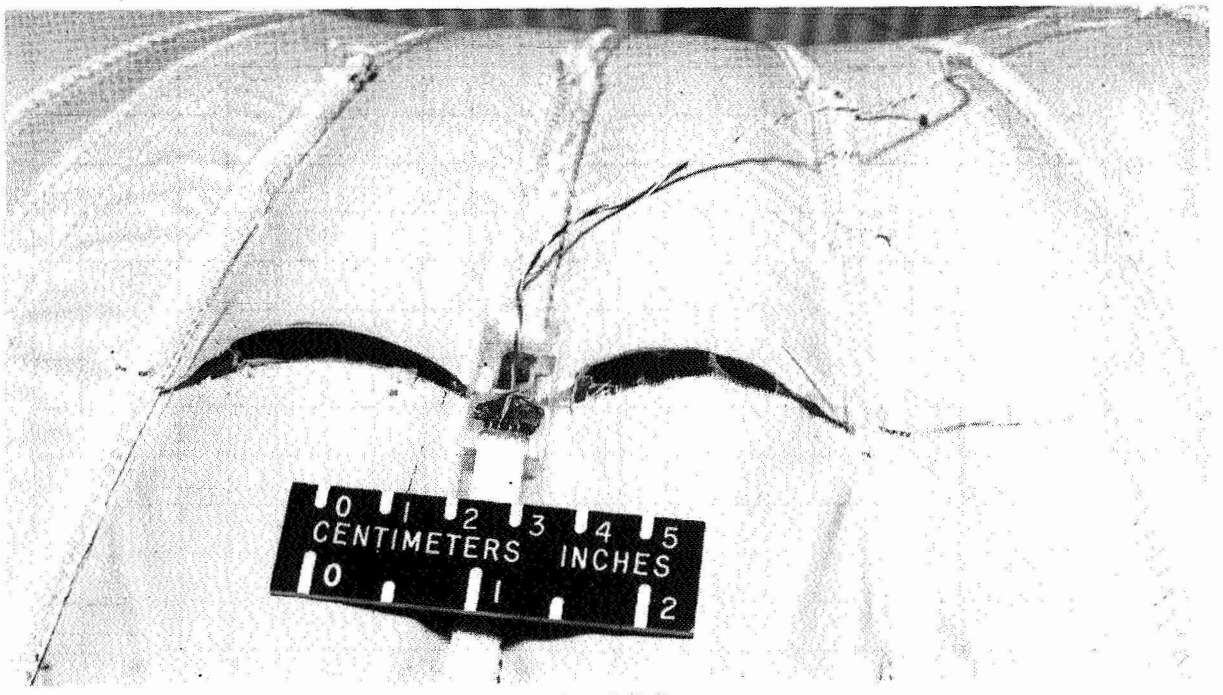

Model 3

L-72-2493

Figure 8.- Photographs of model failure.

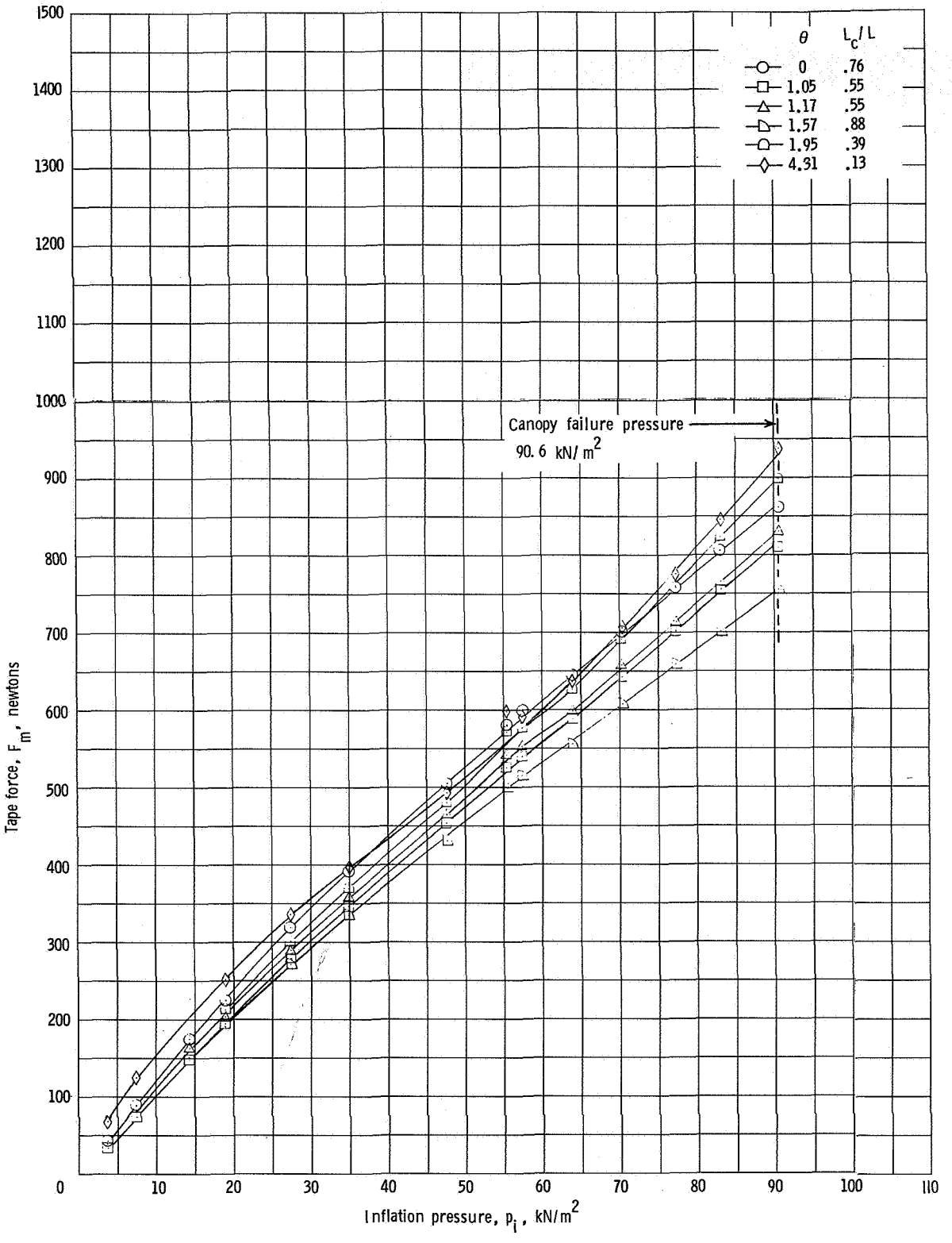

(a) Model 1. Bias cut, single tape.

Figure 9.- Forces in meridional tape for three model configurations.

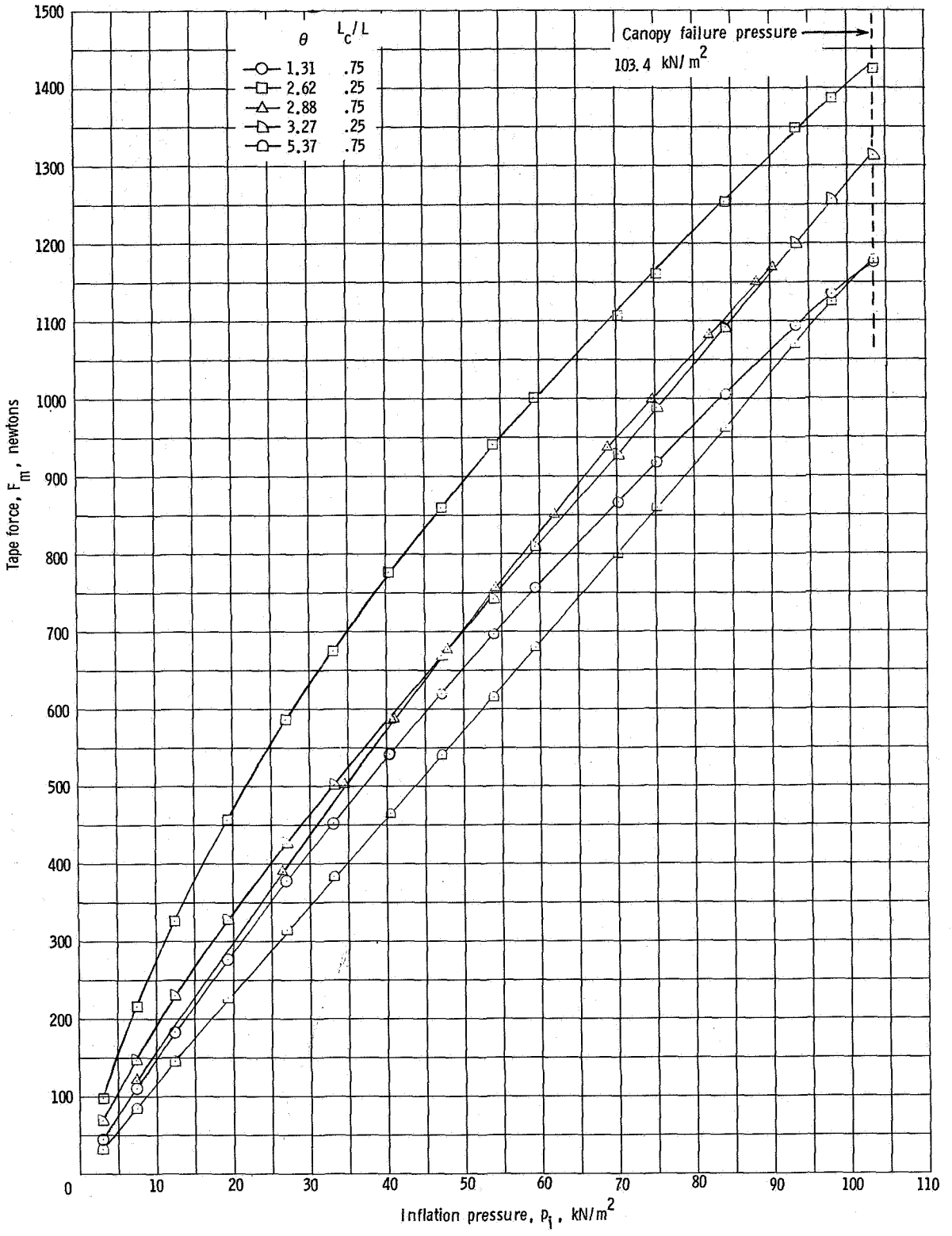

(b) Model 1A. Tapes doubled.

Figure 9.- Continued.

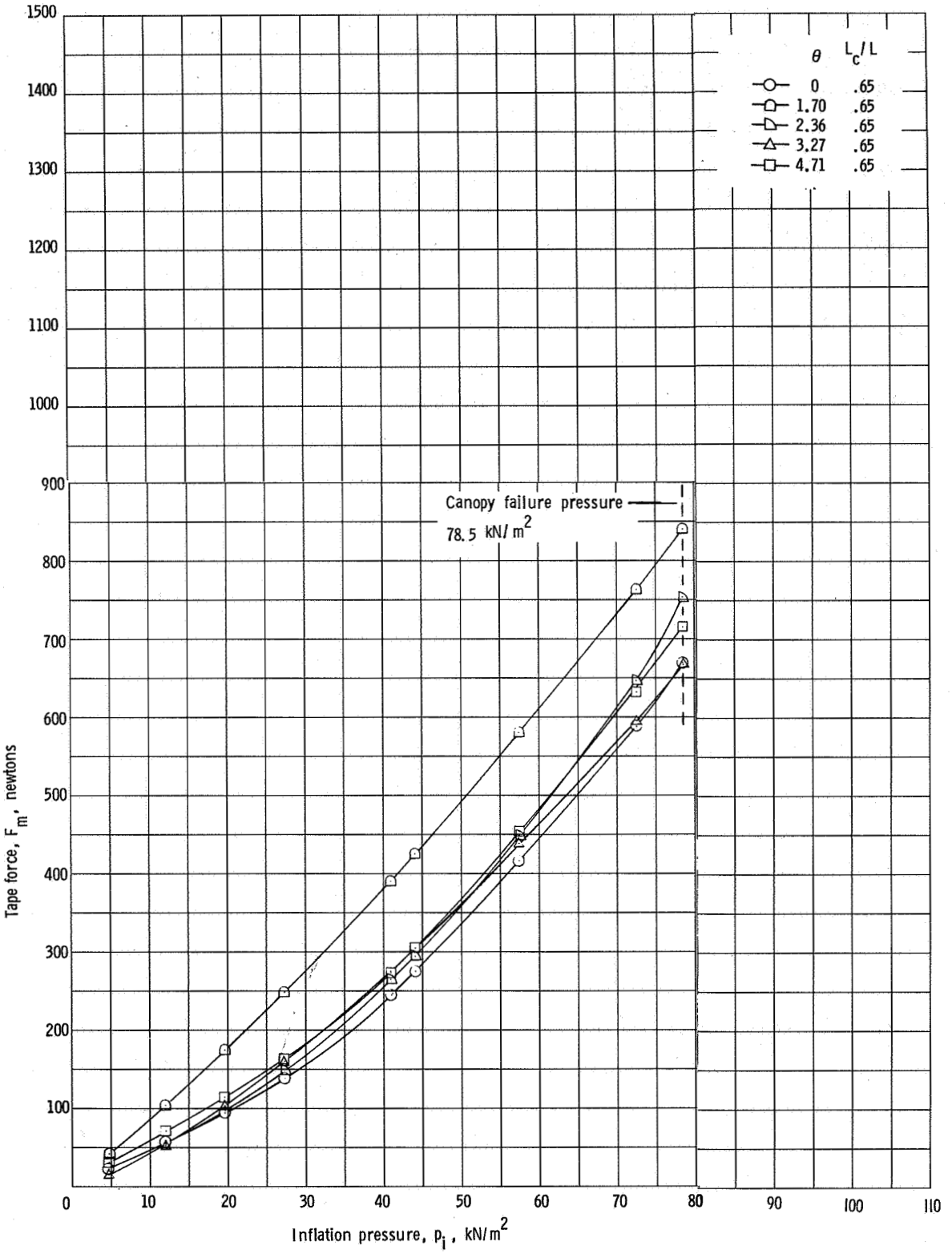

(c) Model 3. Unbiased fabric; single tapes.

Figure 9.- Continued.

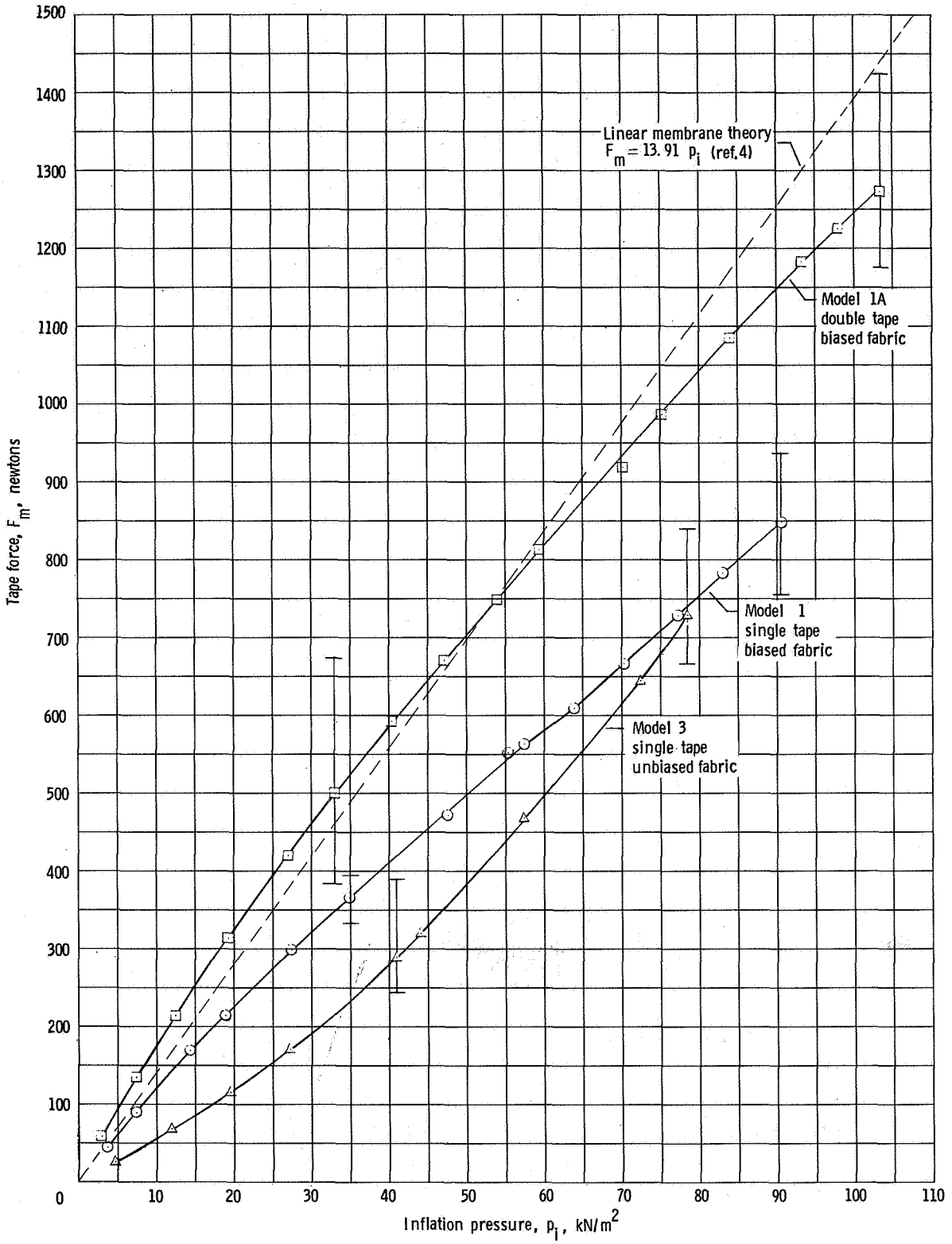

(d) Average tape force for three model configurations.

Figure 9.- Concluded.

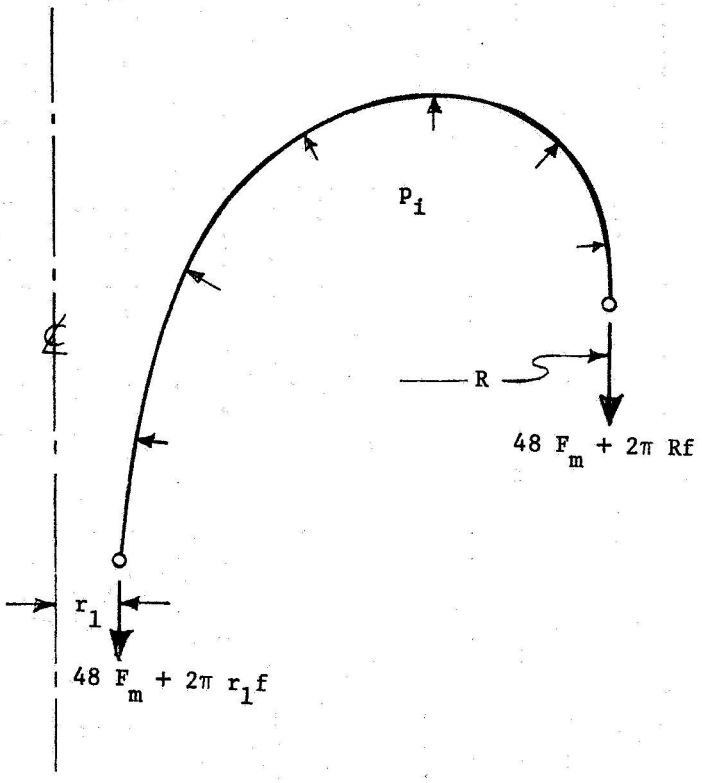

Equilibrium equation:

$$f = \frac{1}{2}\left[p_i\,(R - r_1) - \frac{96\,F_m}{10^3\,\pi(R + r_1)}\right] = .303\,p_i - .0196\,F_m$$

Figure 10.- Vertically directed components of inflation pressure loading on canopy.

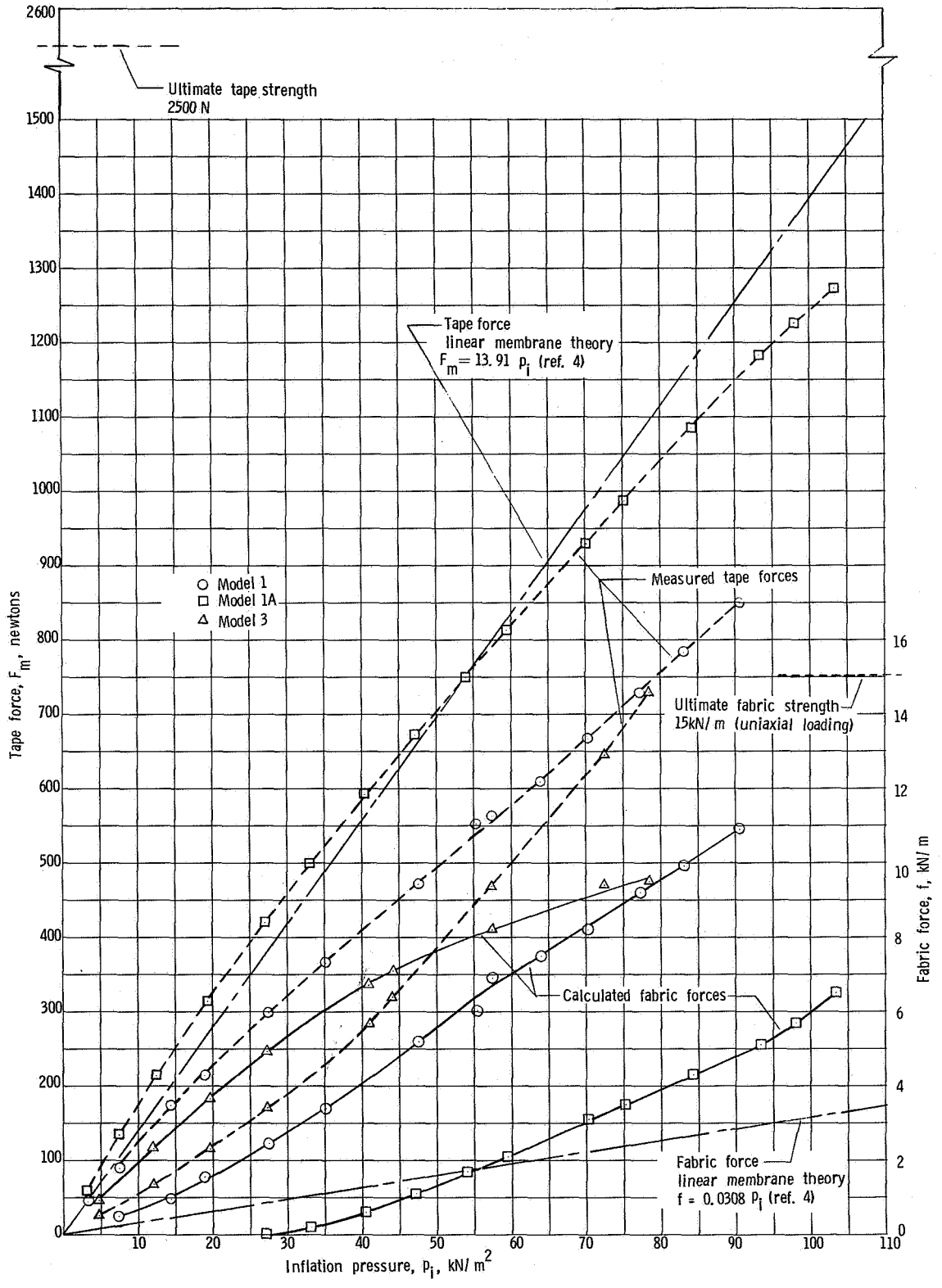

Figure 11.- Forces in fabric for three model configurations.

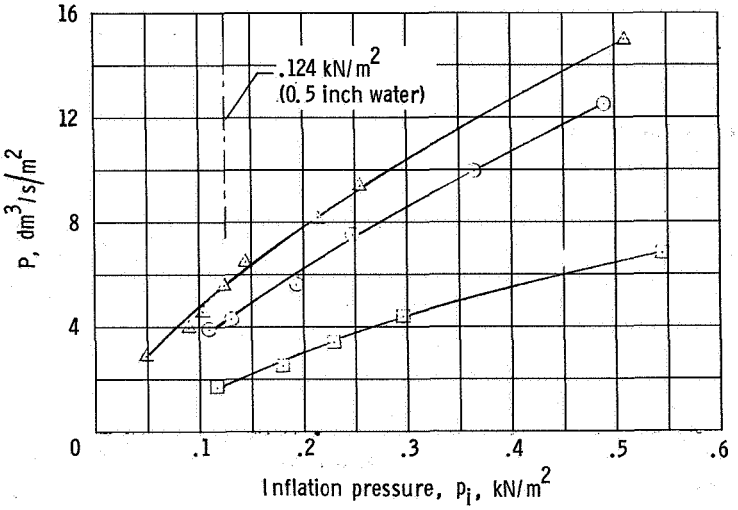

(a) Low inflation pressure.

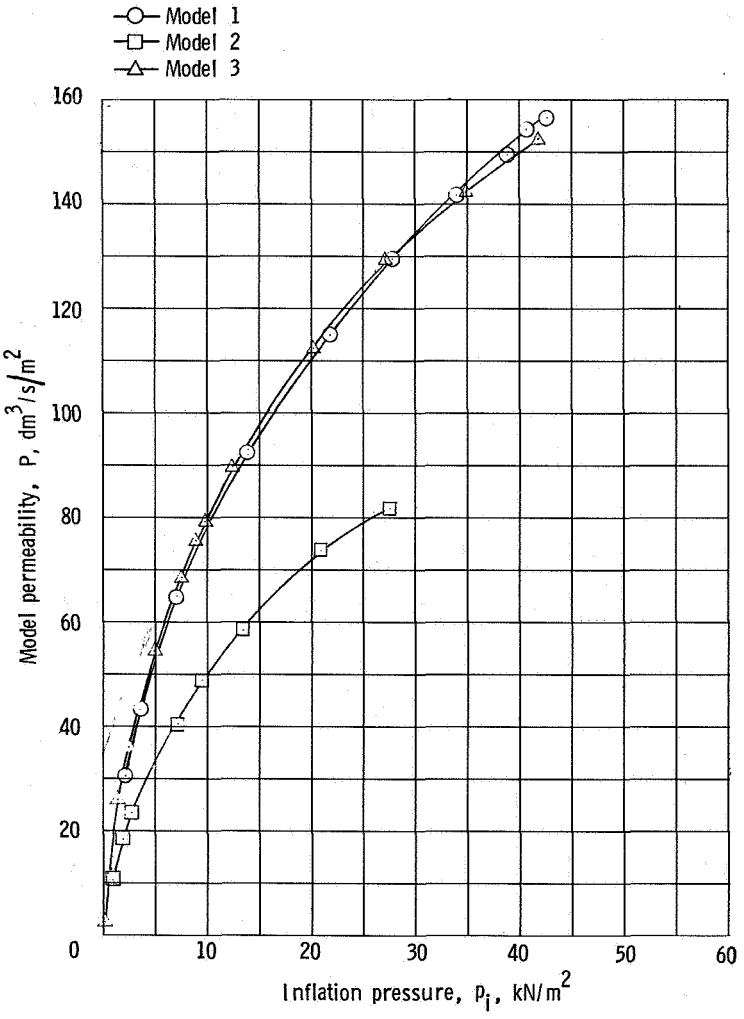

(b) High inflation pressure.

Figure 12.- Permeability of three models at sea-level external pressure.

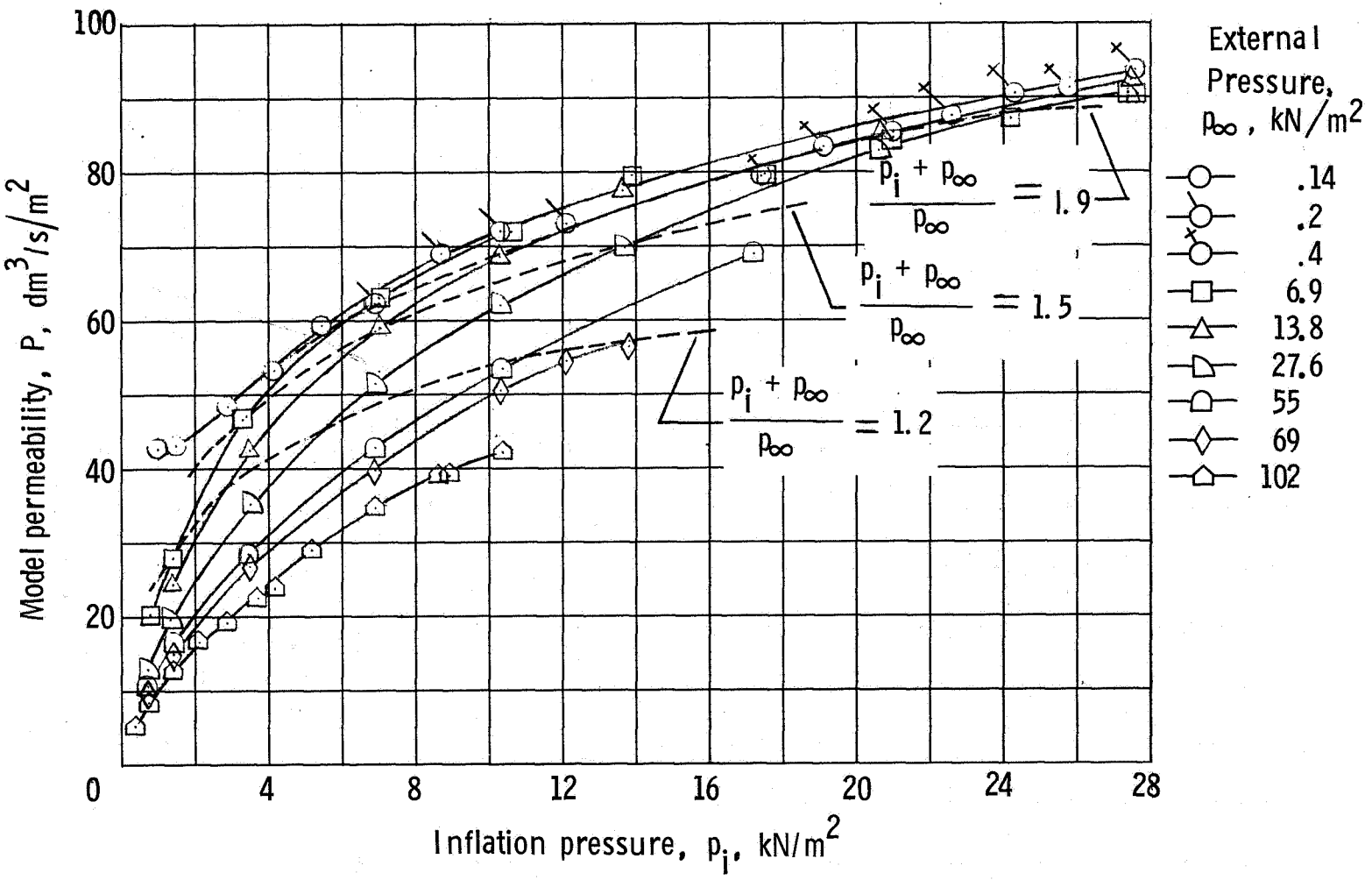

Figure 13.- Permeability at external pressures less than 1 atmosphere. Model 2.

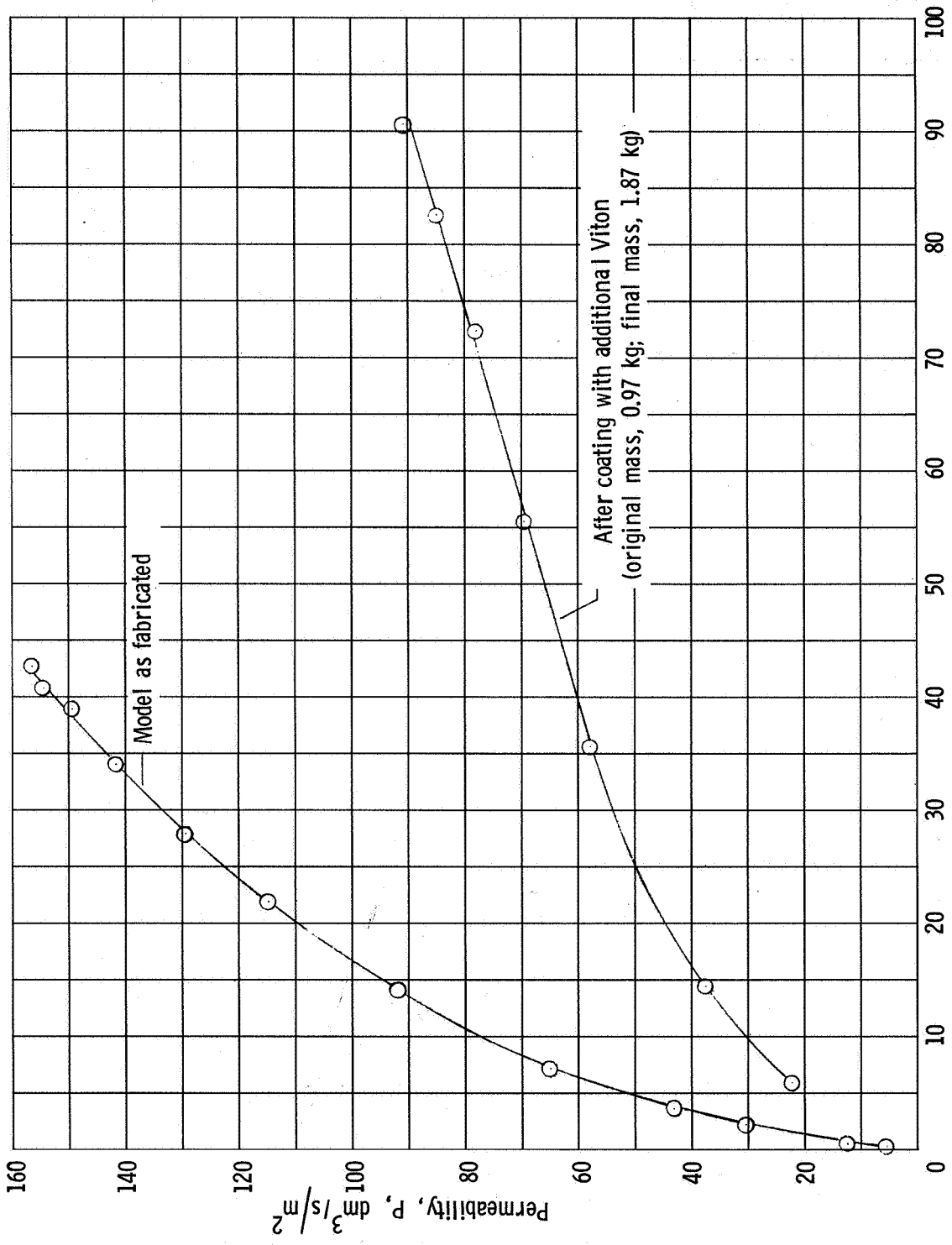

Figure 14.- Effect of Viton coating on model permeability. Model 1.

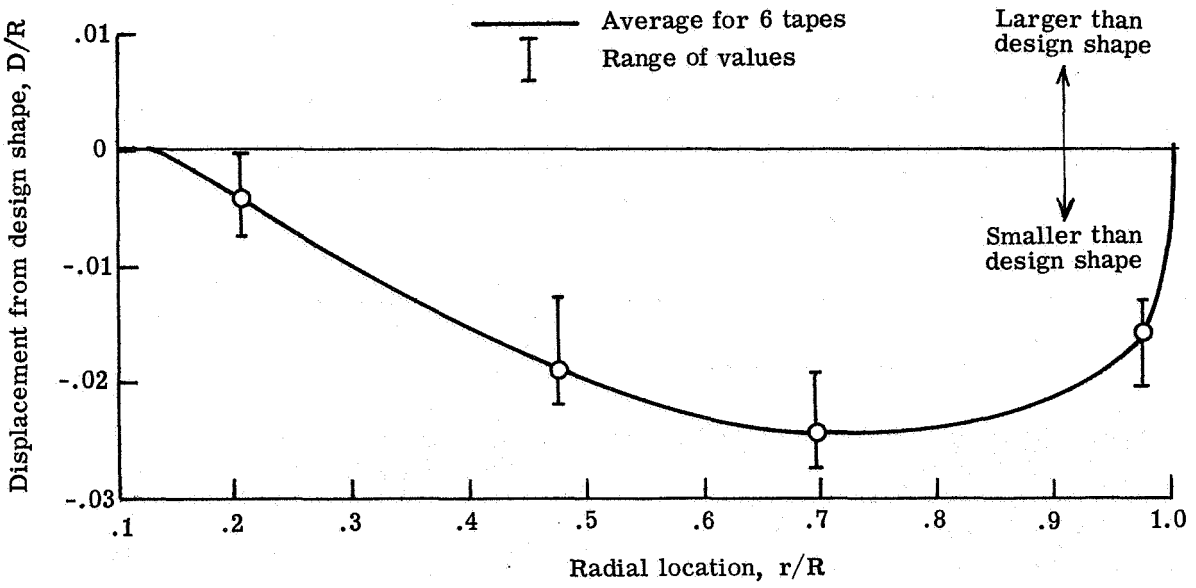

(a) Average measurements along meridional tapes.

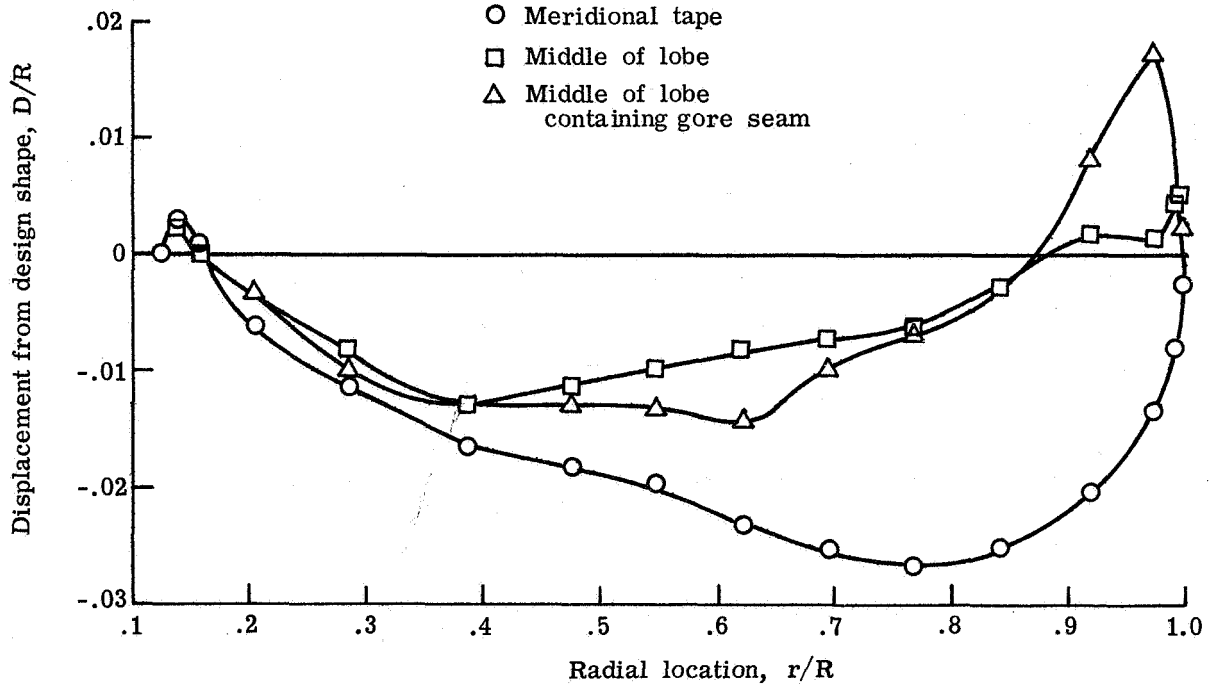

(b) Measurements along three typical stations.

Figure 15.- Deviation of canopy surface from the design shape. p_i = 13.8 kN/m^2; model 1.

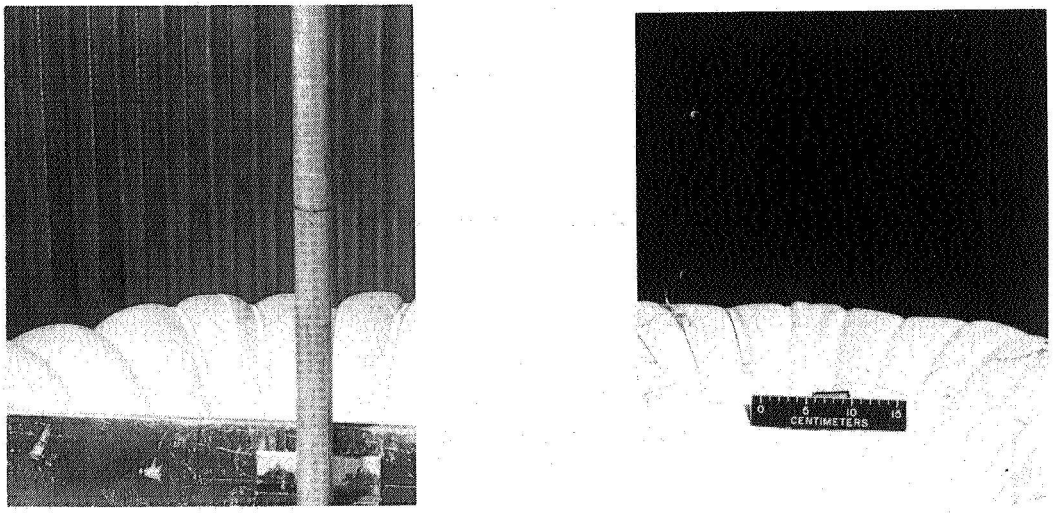

Model 1 Model 3

L-72-2494

Figure 16.- Photographs comparing lobing of unbiased (model 1) and biased models at $p_i = 1\ kN/m^2$.

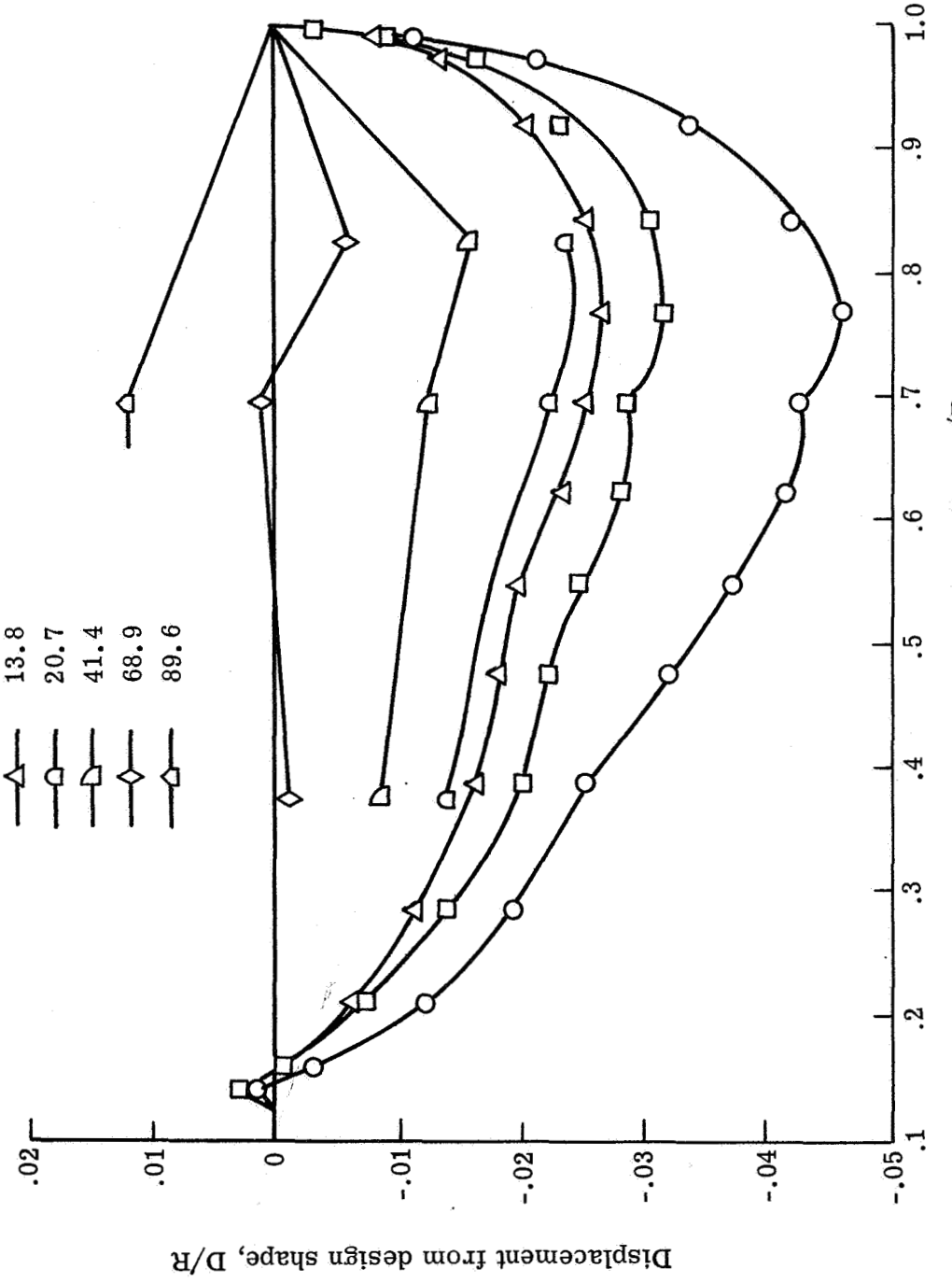

Figure 17.- Measurements along a meridional tape for several pressures. Model 1.

1. Report No.	2. Government Accession No.	3. Recipient's Catalog No.
NASA TN D-6929		

4. Title and Subtitle	5. Report Date
STATIC STRUCTURAL TESTS OF A 1.5-METER-DIAMETER FABRIC ATTACHED INFLATABLE DECELERATOR	October 1972
	6. Performing Organization Code
7. Author(s)	8. Performing Organization Report No.
Conrad M. Willis and Martin M. Mikulas, Jr.	L-8389
	10. Work Unit No.
9. Performing Organization Name and Address	502-32-04-04
NASA Langley Research Center Hampton, Va. 23365	11. Contract or Grant No.
	13. Type of Report and Period Covered
12. Sponsoring Agency Name and Address	Technical Note
National Aeronautics and Space Administration Washington, D.C. 20546	14. Sponsoring Agency Code

15. Supplementary Notes

16. Abstract

Meridional tape forces, permeability, and change in model contours were measured on the aft half of a 1.5-m-diameter attached inflatable decelerator (AID). Inflation pressures up to 103 kN/m^2 and external pressures of 0.14 to 102 kN/m^2 were used. The results indicated that the model stresses were near the desired isotensoid condition. Future AID designs should consider both stiffness and strength of the meridional tapes to obtain the optimum division of load between tapes and fabric. Permeability of pressurized fabric structures is a few orders of magnitude higher than that obtained in the standard low-pressure test on material specimens.

17. Key Words (Suggested by Author(s))	18. Distribution Statement
Reentry vehicles Deceleration Inflatable structures Fabrics Permeability	Unclassified – Unlimited

19. Security Classif. (of this report)	20. Security Classif. (of this page)	21. No. of Pages	22. Price*
Unclassified	Unclassified	31	$3.00

*For sale by the National Technical Information Service, Springfield, Virginia 22151

"The aeronautical and space activities of the United States shall be conducted so as to contribute . . . to the expansion of human knowledge of phenomena in the atmosphere and space. The Administration shall provide for the widest practicable and appropriate dissemination of information concerning its activities and the results thereof."

—NATIONAL AERONAUTICS AND SPACE ACT OF 1958

NASA SCIENTIFIC AND TECHNICAL PUBLICATIONS

TECHNICAL REPORTS: Scientific and technical information considered important, complete, and a lasting contribution to existing knowledge.

TECHNICAL NOTES: Information less broad in scope but nevertheless of importance as a contribution to existing knowledge.

TECHNICAL MEMORANDUMS: Information receiving limited distribution because of preliminary data, security classification, or other reasons.

CONTRACTOR REPORTS: Scientific and technical information generated under a NASA contract or grant and considered an important contribution to existing knowledge.

TECHNICAL TRANSLATIONS: Information published in a foreign language considered to merit NASA distribution in English.

SPECIAL PUBLICATIONS: Information derived from or of value to NASA activities. Publications include conference proceedings, monographs, data compilations, handbooks, sourcebooks, and special bibliographies.

TECHNOLOGY UTILIZATION PUBLICATIONS: Information on technology used by NASA that may be of particular interest in commercial and other non-aerospace applications. Publications include Tech Briefs, Technology Utilization Reports and Technology Surveys.

Details on the availability of these publications may be obtained from:

SCIENTIFIC AND TECHNICAL INFORMATION OFFICE

NATIONAL AERONAUTICS AND SPACE ADMINISTRATION

Washington, D.C. 20546